Target Isolation and Enhancement through Coherent Multi-View Vital-Doppler Detection

Christopher Williams, Syed Doha Uddin, Changzhi Li

Department of Electrical and Computer Engineering, Texas Tech University, Lubbock, TX, USA

Christopher.williams@ttu.edu, syed-doha.uddin@ttu.edu, changzhi.li@ttu.edu

***Abstract*—Doppler Radar has long been considered for use in biomedical applications due to its ability to detect µm-scale displacements. In these cases, a common concern is the ambiguity introduced in vital sign detection caused by clutters, both moving and stationary. This work proposes using multiple radars with coherent multi-view detection to reduce the impact of moving clutter and other factors, such as fundamental harmonics, on vital sign detection.**

Keywords—Doppler, radar, multi-view, cross-correlation.

I. INTRODUCTION

Vital sign sensing using radar technology has been an area of interest in the scientific community since the late 90s [1] due to the non-invasive nature of radar sensing. Because of this nature, there has been an uptick in the interest in using radars as a form of long-term continuous health monitoring [2]. In most cases of radars being used for vital sign recovery, a continuous wave (CW) interferometric radar, also known as Doppler radar, has been used due to its inherent higher sensitivity to micro-Doppler motions [3]. These devices allow for the recovery of micromotions through their quadrature outputs of in-phase and quadrature ac information. On the other hand, the ability of these radars to sense micromotions accurately makes them susceptible to other environmental factors. These factors can range from moving clutters, such as fans, to non-ideal viewing angles of a target. These elements cause an overall decrease in the signal-to-noise (SNR) of the received signal, which can lead to false readings from moving clutters because their spectral peak is higher than the target's. The characteristics of these elements make these systems more prone to error in more complex environments in comparison to a research lab. To combat this, multiple methods have been proposed to relieve the issue of clutters, either moving or stationary, from adaptive filtering algorithms [4] to the use of different radar architectures [5]. The use these kinds of methods increases the confidence in the recovered signals but carries a relatively large overhead compared to interferometric radar in the processing or hardware. In the case of using complex filtering approaches, the overhead is seen in terms of time between receiving data and reporting results, as well as inherent difficulties in making sure the filter retains all pertinent information. On the other hand, changing the radar's hardware from a conventional interferometric radar to a different scheme, such as frequency-modulated continuous wave radar, introduces more room for hardware inaccuracies and reduces the overall sensitivity due to the need for preprocessing before target motion extraction. This change in hardware also increases the overall cost of the device due to the hardware requirements needed to support these more complex transmission schemes compared to Doppler radars. Even in the case where these hardware changes are implemented, biomedical radar still faces the challenge of excessive noise caused by the environment. Another route to address this issue is through the use of multiple radars working coherently to detect a scenario [6]. The benefits provided by a numerous radar approach includes the ability to capture multiple views of a target and innately increase the sensitivity of a sensor setup. Previous works utilizing multiple radars have needed synchronization across radars to properly function. This paper proposes a novel use of a sensor fusion-based multi-radar setup that leverages the cross-correlation method to address the inherent sensitivity to environmental factors, such as random body movement, moving clutter, and environmental noise, to which conventional CW micro-doppler detection processes are subject to. This setup does not require synchronization between the radars in use, allowing for the generalization of the sensing setup across a multitude of scenarios.

The authors wish to acknowledge Rahm Sensor Development and the National Science Foundation (NSF) for funding support under Grant ECCS- 2030094.

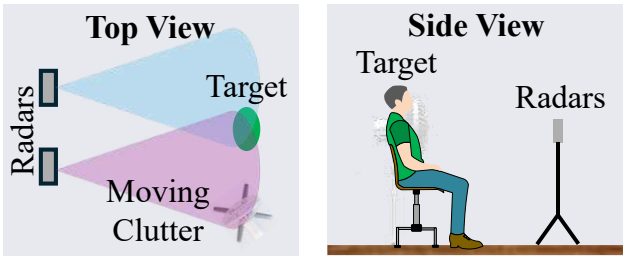

Fig. 1: Example scenario involving a sitting person with adjacent moving clutter being observed by two radars, radar A (topmost) and radar B (bottommost), in which the proposed system is greatly impactful to the ability to detect the vibrations of the target.

II. THEORY

A. Multi-View Radar Scenario

The key behind a multi-view based approach comes from CW Doppler radar detection theory. In the case of Doppler detection, the radar receives a superposition of all the moving targets in its field of view. The complex signal of the radar baseband output can be represented as [7]

$$S(t)_m = I(t) + i \cdot Q(t) = A_\theta \left(\cos\left(\frac{4\pi}{\lambda} \cdot \sum_k x_k(t) + \varphi_k\right) + i \cdot \sin\left(\frac{4\pi}{\lambda} \cdot \sum_k x_k(t) + \varphi_k\right)\right) + DC_{IQ}. \quad (1)$$

2024 IEEE SENSORS | 979-8-3503-6351-7/24/$31.00 ©2024 IEEE | DOI: 10.1109/SENSORS60989.2024.10784984

Where the superposition of the moving targets in the radar's field of view is denoted by the summation of the radial displacement over time ($x_k(t)$) of each target and the phase noise (φ_k) generated at each target. The combination of these two properties inherent to the target is then multiplied by the round-trip length to the target divided by the wavelength of the transmitted signal (λ) creating the received and down-converted information related to the target.

Building off this, it is possible to get utterly different noise profiles of the same target by using multiple radars with multiple different viewing angles toward the target. This is because both differences in the position of the radars and their viewing angle cause a change in the amplitude of the returned signals (A_θ) and what type of signals are captured by the radars. The change in amplitude is due to most targets not having a uniform radar cross-section, creating angles where there are better and worse returns to a radar. An example of a scenario like this is depicted in Fig. 1. The figure shows that radar A can see moving clutter, depicted as a fan, as well as the target motion. At the same time, radar B can only see the target of interest and its motion. A scenario like this causes the radars to have a unique signal and noise spectrums from each other and different views of a target's unique radar cross-section profile.

B. Cross-Correlation Method

Based on these unique spectrums, we can use the cross-correlation method to extract common frequency components across the radars while discounting their unique noise sources. The process of cross-correlating the two signals results in peaks appearing where the signals share maximums or minimums in the signals due to the process of time shifting and multiplication. The mathematical expression for the discrete signal cross-correlation used can be seen in [8]

$$(S_1 \star S_2)[n] = \sum_{m=-M}^{M} \overline{S_1[m-n]} \cdot S_2[m]. \qquad (2)$$

where S_X (X = 1 or 2) denotes a specific complex signal from one radar. The bar over $S_1[m-n]$ denotes the use of the complex conjugate of those elements during the process of cross-correlation. This process results in the recovery of similar frequencies across the two signals while rejecting the peaks inconsistent across each radar. These resulting elements are called similarity coefficients and denote at what delay (n) the signals are most similar to each other.

Returning to the scenario discussed in section II. A This allows for capturing the low-amplitude vibrations of the target while attenuating the clutter usually seen in biomedical applications. It also enhances the overall signal-to-noise (SNR) ratio in the recovered vital sign signal. The increase in SNR, due to the attenuation of the noise factors, affords greater accuracy and certainty in the recovered data. To make use of this, the algorithm proposed in this work utilizes the cross-correlation in the time domain across each radar's *I/Q* channels to isolate the desired signal across multiple radars and reduce the contributions from noise factors, such as moving clutter and unique harmonics.

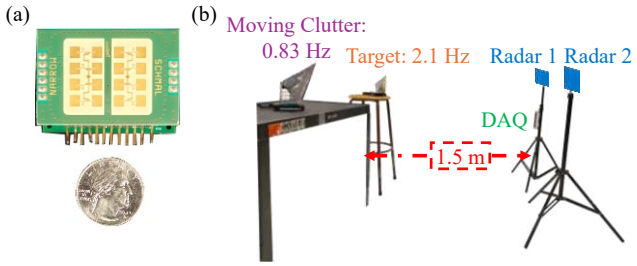

Fig. 2: (a) Size comparison of the 24 GHz IPS-154 modules used for radar 1 and 2 with a quarter for scale, and (b) the experimental setup for a target in the presence of moving clutter.

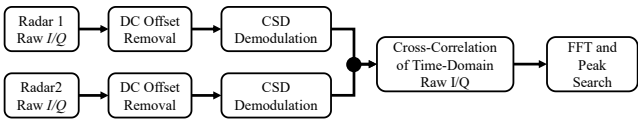

Fig. 3: Data processing flowchart of the proposed method with example plots of the data.

III. Experimental Results

To verify the usefulness of the process outlined in section II, experiments were conducted using two 24 GHz Doppler radars. The radars used are composed of InnoSenT IPS-154 24 GHz Doppler radar front-end modules that have a quadrature down conversion architecture connected to an off-board baseband circuit. The baseband circuitry used with the front-end radar modules was designed in-house. It consists of two single-stage ac-coupled inverting amplifiers providing 20 dB of gain for each *I* and *Q* channel. The overall size of the module is relatively small, and a comparison to the size of a quarter is illustrated in Fig. 2(a). An NI USB 6210 DAQ was connected to the radar modules to capture the received baseband signals. The experimental setup follows the scenario outlined in Fig. 1 and consists of two actuators set up in front of the radar setup. To verify the ability to isolate moving clutter in a multi-view scenario, the two actuators had different frequencies, one oscillating at 0.83 Hz and one at 2.1 Hz. These frequencies were chosen because they do not possess harmonics that land on the fundamentals of the other frequencies. An image of the complete experimental setup is illustrated in Fig. 2 (b).

A. Target Isolation

To prepare the raw data for post-processing, the dc offset (or mean) of the data was removed. This is necessary due to the baseband circuitry used being ac coupled to the radio frequency front-end. The ac-coupling of the baseband causes the dc information seen directly out of the DAQ to be a combination of the dc information generated by the target and spurious dc information generated by the baseband circuitry. This combination causes the dc information contained in the ADC sampled data to be corrupted. Therefore requiring the removal of the dc information. After the dc removal, the I and Q data for each radar is then combined through complex signal demodulation (CSD) to combine the phase information contained in the individual I and Q channels from a radar [7]. To compare the results with and without the cross-correlation, a Fast Fourier Transformation (FFT) was applied to the combined complex signals of each radar to convert the time-domain raw signals to frequency-domain signals and verify the initial signal

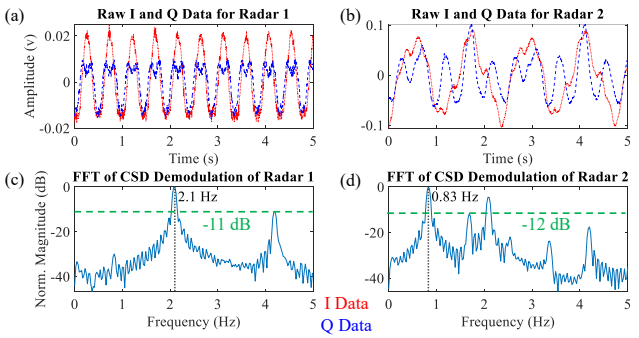

Fig. 4: Raw radar *IQ* signals from radar 1 (a) and 2 (b). The FFTs of the CSD signals from radar 1(c) and 2 (d). The green line on each graph depicts the relative power of the dominant frequency's first harmonic.

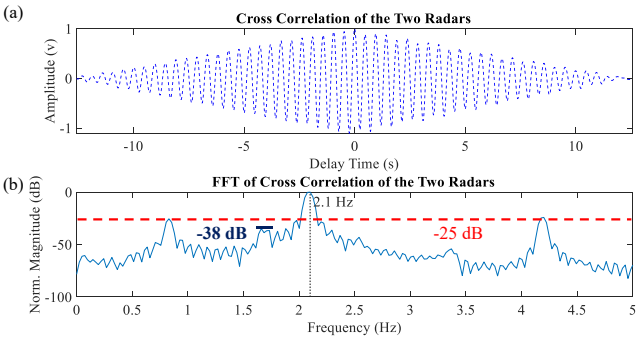

Fig. 5: (a) Time domain results after cross-correlation between two 24 GHz radars and (b) FFT results of the cross-correlation. The red line in the FFT results depicts the relative power level of the dominant frequency's first harmonic. The dark blue line on the other hand highlights the moving clutters first harmonic which is highly attenuated after cross-correlation.

issues. A flow chart depicting the overall signal flow for the experiment is shown in Fig 3. The signal processing depicted in the figure was done in MATLAB. Fig. 4. (a) and (b) illustrates the raw *I* and *Q* channel data from the radars. The resultant frequency spectrum from the FFT of the combined data is shown in Fig. 4. (c) and Fig. 4. (d). The frequency domain data was converted to dB to better illustrate the difference before and after cross-correlation. For both cases, the properties of the FFT, including the number of points used for the FFT, were taken as the same to lower the divergence in the results perceived after the FFT. This is important because the FFT properties have a direct relationship with the signal power and the frequency of spreading that can be caused by the FFT properties. This concept is the same as the resolution bandwidth on a spectrum analyzer and the effects it has on experimental results. As can be seen from the figure, in the multi-view scenario, radar 2 sees the moving clutter at 0.83 Hz as the dominant frequency of the target, while radar 1 sees the target's 2.1 Hz as the dominant frequency. This poses target detection issues due to the ambiguity in the target's motion across radars.

The cross-correlation method was applied to the time domain CSD data for each radar to address this issue. This process during the post-processing flow is shown in Fig. 3. The cross-correlation of the two modules generates a set of similarity coefficients between the two radar signals relative to the time shift of one signal to the other during the cross-correlation process shown in equation (2). The resultant similarity coefficients between radar 1 and radar 2 are shown in Fig. 5. (a). After this, a second FFT was taken of the cross-correlated data to see the effects on the moving clutter and target isolation. The frequency domain results of the cross-correlation are presented in Fig. 5. (b). From Fig. 5. (b), it can be seen that the magnitude of the moving clutter was reduced significantly, from being the dominant frequency in radar 2 to being at the same relative dB level as the first harmonic of the target's 2.1 Hz frequency at -25 dB. This reduction can be attributed to multiple factors related to the cross-correlation method. As can be seen from the figure, the detection of the target's motion has much higher certainty than before due to the decrease in the magnitude of the non-target peaks.

B. Harmonic Reduction

Another result seen from the cross-correlation is in the attenuation of the harmonic of the target's frequency and the moving clutters'. This reduction is due to differences in the magnitude and commonalities between the harmonic components of each radar. From Fig. 4. (a) and (b), it can be seen that while radar 1 sees the moving clutter at -30 dB, the harmonic generated by the moving clutter is lost in the frequency roll off of the dominant frequency of 2.1 Hz in the case of radar 1. This causes the harmonic of the 0.83 Hz after cross-correlation to be largely attenuated in the cross-correlation result (appearing at -38 dB) due to its similarity coefficient being lower. The same holds true for the harmonic of the target's frequency, at 4.2 Hz, being attenuated from -11 dB in radar 1 to -25 dB after cross-correlation. The relative magnitude of the harmonic after cross-correlation from the fundamental tone to the harmonic is not only decreased due to the similarity mismatch but also because of the increase in both the strength and length of the fundamental after cross-correlation. The combination of these two factors can be seen in the overall reduction in relative magnitude seen in Fig. 5(b). These effects also hold true across multiple scenarios due to the experimental radars having zero synchronization between them in either time or the precise frequency of their local oscillators.

IV. CONCLUSION

In conclusion, a multi-view radar sensor set up to increase the isolation and reduce the harmonics of a target has been proposed, leveraging the cross-correlation between independent radar sensors. Experimental analysis has been carried out using multiple actuators to successfully demonstrate the algorithm's target isolation capabilities. This system allows for the recovery of the fundamental frequency in the presence of moving clutter while attenuating the harmonics caused by both. The generality of this process allows for the deployment of this system in a multitude of scenarios due to the sensing setup being actualized without any needed synchronization between the radars or other extraneous setup. In the future, a more robust and quantitative study will be carried out to analyze the effects the proposed approach has on both noise and other interference under various scenarios.

REFERENCES

[1] E. F. Greneker, "Radar sensing of heartbeat and respiration at a distance with applications of the technology," in *Radar Systems (RADAR 97)*, Edinburgh, UK: IEE, 1997, pp. 150–154. doi: 10.1049/cp:19971650.

[2] Y. Qiu, M. Yamamoto, S. Takamatsu, and T. Itoh, "A Map Feature Fusion Based Artifact Removal Method for Non-Contact Vital Sign Detection with a Single FMCW Radar," in *2023 IEEE SENSORS*, Vienna, Austria: IEEE, Oct. 2023, pp. 1–4. doi: 10.1109/SENSORS56945.2023.10324886.

[3] S. Dong *et al.*, "A Review on Recent Advancements of Biomedical Radar for Clinical Applications," *IEEE Open J. Eng. Med. Biol.*, pp. 1–18, 2024, doi: 10.1109/OJEMB.2024.3401105.

[4] Y. Wang *et al.*, "A Novel Non-Contact Respiration and Heartbeat Detection Method Using Frequency-Modulated Continuous Wave Radar," *IEEE Sens. J.*, vol. 24, no. 7, pp. 10434–10446, Apr. 2024, doi: 10.1109/JSEN.2024.3351274.

[5] L. Lu, X. Ma, Y. Liang, Z. Liu, X. Fan, and L. Li, "A 60-GHz Hybrid FMCW-Doppler Radar for Vibration Detection With a Robust I/Q Calibration Method," *IEEE Sens. J.*, vol. 22, no. 21, pp. 20464–20474, Nov. 2022, doi: 10.1109/JSEN.2022.3206107.

[6] K. Han and S. Hong, "Differential Phase Doppler Radar With Collocated Multiple Receivers for Noncontact Vital Signal Detection," *IEEE Trans. Microwave Theory Techn.*, vol. 67, no. 3, pp. 1233–1243, Mar. 2019, doi: 10.1109/TMTT.2018.2884406.

[7] C. Li and J. Lin, "Random Body Movement Cancellation in Doppler Radar Vital Sign Detection," *IEEE Trans. Microw. Theory Tech.*, vol. 56, no. 12, pp. 3143–3152, Dec. 2008, doi: 10.1109/TMTT.2008.2007139.

[8] L. R. Rabiner and B. Gold, Theory and Application of Digital Signal Processing. India: Pearson India Education Services, 2016.